

Microstrip Patch Antenna Design at 10 GHz for X Band Applications

Mehmet Karahan^{1,*}, Mertcan Inal², Alperen Dilmen³, Furkan Lacinkaya⁴, Ahmet Nuri Akay⁵ and Cosku Kasnakoglu⁶

^{1, 2, 3, 4, 6}TOBB University of Economics and Technology, Electrical and Electronics Engineering, Turkey

⁵TOBB University of Economics and Technology, Materials Science and Nanotechnology Engineering, Turkey

*Corresponding author

Abstract

Microstrip patch antennas are used in satellite imaging systems, wireless communication equipment, military radios, GPS (Global Positioning System) and GSM (Global System for Mobile Communications) applications. Its advantages are its small size and light weight, thin structure, low power consumption, use in dual frequency applications, and patching in various geometric shapes. Developing technology has facilitated and accelerated the production of microstrip antennas. In this study, microstrip antenna design operating at 10 GHz frequency for X band applications has been made. X band is used for air traffic control, weather traffic control, vessel traffic control, defense tracking and vehicle speed detection, terrestrial communications and networking, space communications and amateur radio. HFSS program was used in antenna design. AWR program was used to find transmission line parameters. In addition, MATLAB program was used to calculate some parameters. First of all, information is given about the working principle of the antenna, the selected dielectric layer and the working frequency. Schematic drawings of the designed antenna were made from above and from the side. S11 reflection coefficient magnitude graphs are drawn below and above the operating frequency. The radiation pattern is drawn for the E-plane and H-plane at the operating frequency. 3-D (dimensional) plot of antenna gain at operating frequency is drawn. The simulations performed have shown that the designed antenna works successfully.

Keywords: antenna radiation patterns, antenna measurements, gain measurement, slot antennas, wireless communication

1. Introduction

Microstrip patch antennas are low profile antennas. They are used in low profile applications at frequencies above 100 MHz [1]. A metal patch mounted at a ground level with a dielectric material in between creates a microstrip [2]. The patch on the upper surface is made of conductive materials such as copper or gold [3]. The geometric shape of the conductor to be used may vary according to the design features. Square, rectangle, ellipse, ring etc. can be used in shapes [4]. Microstrip antennas could be used in different applications such as aircrafts, spacecrafts, satellites, missiles, mobile radios, and wireless communications [5]. Microstrip patch antennas can also be used in unmanned aerial vehicles due to its miniaturized dimensions [6].

Rana et al. designed a microstrip patch antenna operating at 2.4 GHz for use in wireless communication [7]. They used CST studio suite program for the design. They achieved low returns and high gain in their designs. Colaco and Lohani developed a microstrip patch antenna

operating at 26 GHz [8]. Since they need high data and high bandwidth, they have developed a design using 5G millimeter wave bands. They used FEKO software for simulation and analysis. Kiani et al. designed a microstrip patch antenna using reconfigurable graphene material. They stressed that changes in the chemical potential of graphene are directly caused by changes in Fermi energy. They used graphene material to adjust the polarization of the microstrip patch antenna. They carried out their simulations in the frequency range of 0.65 to 0.7 THz [9]. Hocini et al. designed a terahertz microstrip patch antenna based on photonic crystals. They obtained best antenna characteristics 0.65 THz. Their proposed antenna had high radiation efficiency as 90.84% [10]. Wang et al. proposed a frequency reconfigurable antenna design. They designed a frequency reconfigurable microstrip patch antenna using graphene film. They used the graphene film in direct contact with the Si/SiO₂ substrate. Their test results showed that center frequency of their antenna was 29.6 GHz when the bias voltage was 0 V and 40 GHz when the bias voltage was 9 V [11]. Ghimire et al. designed a slot-line-based microstrip patch antenna. They fabricated and analyzed this antenna inside a far-field anechoic chamber. The measured results showed that antenna had a frequency range of 8.5 to 11 GHz [12]. Benlakehal et al. developed a graphene based microstrip patch antenna in 0.636 THz band. They developed a 1x2 microstrip patch antenna array based on photonic crystals. They obtained a high gain as 11.53 dB [13].

In this research, a microstrip patch antenna design operating at 10 GHz frequency was carried out. The microstrip patch antenna design was developed for X band applications. A design with high gain, small size, thin structure, light weight and low power consumption has been achieved. A computer program called HFSS was used for antenna design. AWR program was used to obtain transmission line parameters. The MATLAB program was used to make the necessary mathematical calculations. At certain intervals of the antenna's operating frequency, S₁₁ reflection coefficient magnitude graphs were drawn. Antenna's radiation pattern is drawn for the E-plane and H-plane at the operating 10 GHz frequency. 3-D plot of antenna gain at operating 10 GHz frequency is shown. The obtained simulation results proved that the designed microstrip patch antenna works successfully.

1.1 Microstrip patch antenna and its excitation

Microstrip is a type of electrical transmission line that can be manufactured using printed circuit board technology and is used to transmit microwave-frequency signals. It consists of a conductive strip separated from the ground plane using a dielectric layer known as the substrate [14]. Many microwave circuit elements such as antennas, synchronizers, filters and power dividers can be made using microstrips. Microstrips are cheaper, lighter and more compact than standard waveguides [15]. Microstrip patch antenna basically consists of a metal ground layer at the bottom, a substrate consisting of dielectric material in between, and a metal patch at the top that provides radiation [16]. A typical microstrip patch antenna is shown in Figure 1.

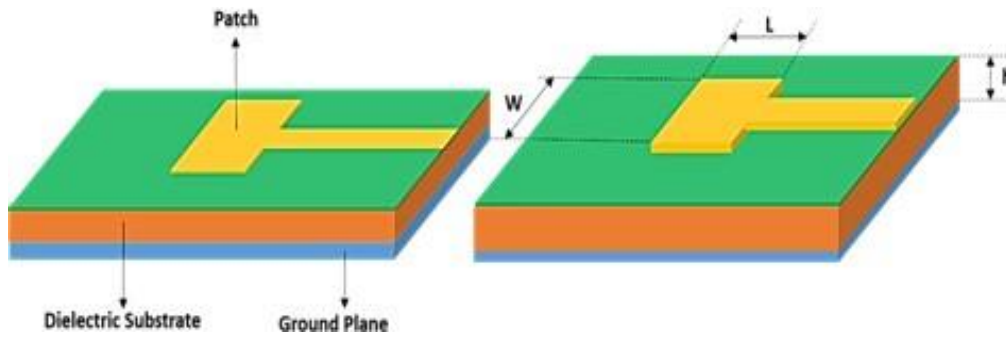


Figure 1: A typical microstrip patch antenna

The dielectric ground with the patches is not magnetic. The small dielectric constant of the dielectric ground causes the fringe areas to increase, which affects the radiation [17]. In general, when designing the antenna, it is preferred that the dielectric constant is between 2.2 and 12 [18]. The length L , width W and thickness H are effective in characterizing this type of antenna.

1.2 Patch antenna excitation

Transmission line feeding, coaxial cable feeding or inset (embedded) feeding can be used for patch excitation [19], [20]. In this research, inset feeding was used due to space constraints. In this method, $Z_{in}(R)$ is pulled to the desired location by starting from the input impedance ($Z_{in}(0)$) when there is no inset [21]. Figure 2 shows the schematic representation of inset feeding. Its formula is given in equation 1.

$$Z_{in}(R) = \cos^2(\pi R/L)Z_{in}(0) \quad (1)$$

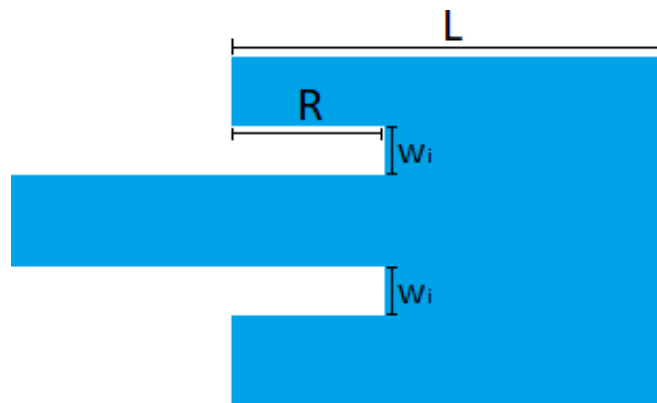


Figure 2: Schematic representation of inset feeding.

1.3 Working principles

Excitation of the conductive patch, on the other hand, causes an electromagnetic wave movement from the edges of the patch to the ground. Waves reflected from the ground propagate into space. The areas formed on the edges of the conductive patch are called fringing areas and this phenomenon is called fringing effect [22]. Figure 3 gives the schematic representation of fringing areas. The radiation of the antenna occurs as a result of this event.

Waves perpendicular to the patch dampen each other and do not radiate, waves fringing from the corners make the radiation.

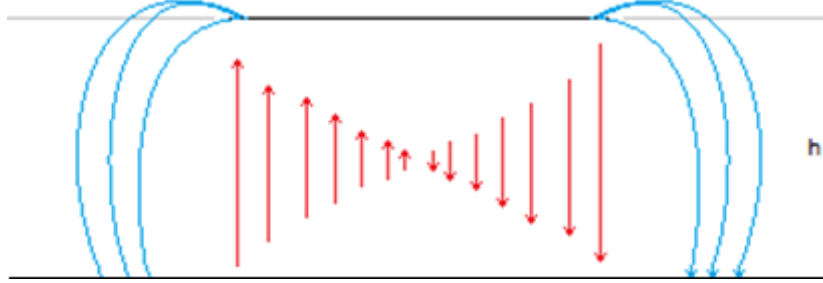


Figure 3: Schematic representation of fringing areas.

2. Design of the Microstrip Patch Antenna

In this section, the operating frequency of the antenna, the selected dielectric layer, and the design procedures are explained. A side and top schematic view of the designed antenna is given.

2.1 Frequency and dielectric layer

It was stated in the design specifications that the communication system uses certain frequencies in the 10-12 GHz range, so 10 GHz within this range was chosen as the center frequency. In the dielectric layer, RO4003 material was chosen because of its high frequency performance, low loss and widespread use in microstrip antenna designs [23]. The dielectric constant of this material is 3.4 and its tangent loss is 0.002 [24].

2.2 Design procedures

In this research, HFSS program was used for simulation and modeling purposes. AWR program is used to organize some graphs and find transmission line parameters. In addition, MATLAB program was used for some calculations.

First of all, the dimensions of the antenna were determined. The operating frequency of the antenna is determined by L (length). The center frequency is calculated approximately as in equation 2, where c is the speed of light.

$$f_c \approx c/2L\sqrt{s_r} = 1/2L\sqrt{\mu_0 s_0 s_r} \quad (2)$$

Equation 3 is obtained by subtracting L from equation 2.

$$L \approx c/2f_c\sqrt{s_r} \quad (3)$$

When the equations were solved using the MATLAB program, L = 7.96 was found. Another parameter of the antenna, w (patch width), is determined by the following formula:

$$w = (c/2f_c)/(\sqrt{2}/(s_r + 1)) \quad (4)$$

When the equations were solved with the MATLAB program, w = 9.94 mm.

Equation 5 was used to calculate the h (height). When this equation was solved with MATLAB, it was found that h = 0.96.

$$(0.0606 \lambda)/(\sqrt{s_r}) \quad (5)$$

As ϵr (dielectric constant) decreases, the effective length of the antenna also changes due to the increase in fringing areas. There may be deviations in f_c (center frequency) due to these changes. Therefore, the antenna effective length (L_{eff}), normalized extension in length (ΔL) and effective dielectric constant (ϵr_{eff}) are additionally calculated below:

$$\epsilon r_{eff} = (\epsilon r + 1)/2 + (\epsilon r - 1)/2[1 + 1.2h/w]^{-1/2} \quad (6)$$

$$\Delta L = 0.142h[(s_{reff} + 0.3)(w/h + 0.264)]/[(s_{reff} - 0.258)(w/h + 0.8)] \quad (7)$$

$$L_{eff} = L + \Delta L \quad (8)$$

When the above equations are solved with MATLAB program, $\epsilon r_{eff} = 3.1417$, $\Delta L = 0.4513$ mm, $L_{eff} = 8.8582$ mm results are found.

In inset (embedded) feeding, the following equation was obtained by using the equation (1) and starting from the input impedance ($Z_{in}(0) = 204.75\Omega$).

$$R = \cos^{-1}\left(\frac{Z_{in}(R)}{Z_{in}(0)}\right)\frac{L}{\pi} \quad (9)$$

Then, using the MATLAB program, $R = 2.6689$ mm was calculated. The width value at the embedded feed was calculated as $w = 0.3313$ mm. For the design of the microstrip line, parameters such as line length, line width, line height were found by using the Microstrip section of the AWR program. These parameters are shown in Figure 4.

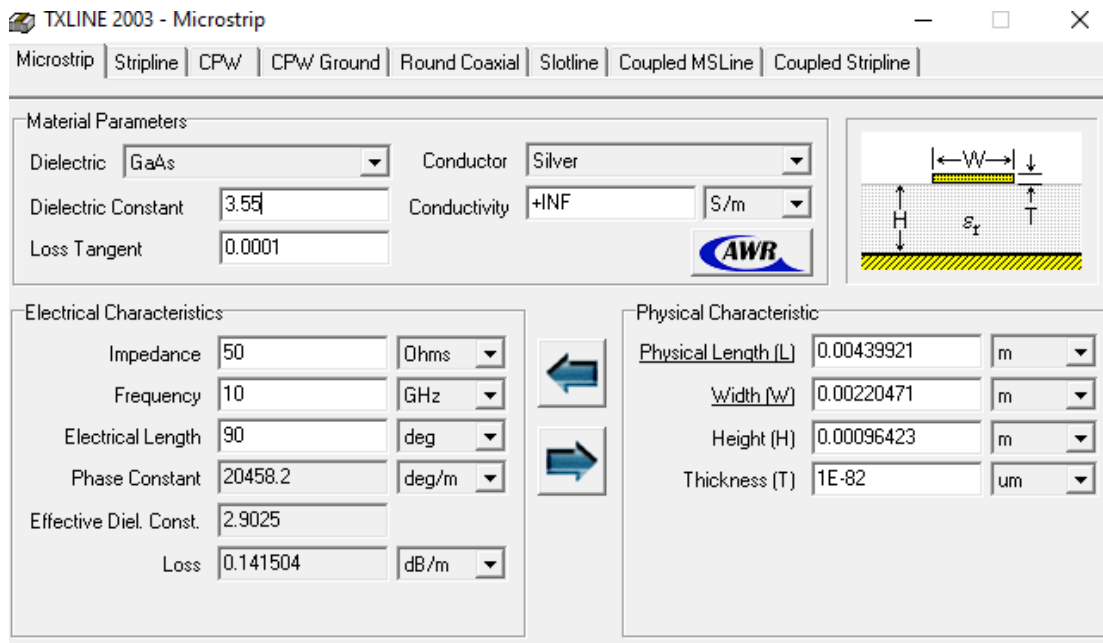


Figure 4: Calculation of microstrip line parameters in AWR.

The parameters of the designed antenna are given in Table 1.

Table 1: Design parameters of the 10 GHz X Band microstrip patch antenna

Working frequency	10 GHz
Wavelength	3 cm
Antenna width	1.6 cm
Antenna length	1.6 cm
Antenna effective length	0.88582 cm
Antenna height	0.0964 cm
Patch length	0.7554 cm
Patch width	0.9938 cm
Patch height	neglected
Dielectric base material	RO4003
Dielectric base dielectric constant	3.4
Effective dielectric constant	3.1417
Dielectric base tangent loss	0.002
Dielectric base height	0.0964 cm
Dielectric base length	1.6 cm
Dielectric base width	1.6 cm
Band width	0.2832 GHz
Gain	6.8 dB
Impedance	64 Ω
Transmission line length	4.399 cm
Transmission line width	2.205 cm
Transmission line thickness	neglected
Transmission line impedance	50 Ω
Embedded feed w	0.03313 cm
Embedded feed R	0.2669 cm

2.3 Schematic drawings of the designed antenna

The designed antenna is shown schematically in Figure 5, showing the design parameters and dimensions. It is seen that the total volume rule (1.6 cm x 1.6 cm x 1 mm) given in the design specifications is followed here. Of the values calculated in Section 3, all except L remained the same. The reason for the change of L is the change of L_{eff} due to the fringing areas, as emphasized earlier. L was found by modifying it with the HFSS program to provide the center frequency as its graph is given in the next sections. The patch and ground plane parts shown in the figure are taken as PEC (perfect electrical conductor), and the thickness of the conductive surfaces is neglected.

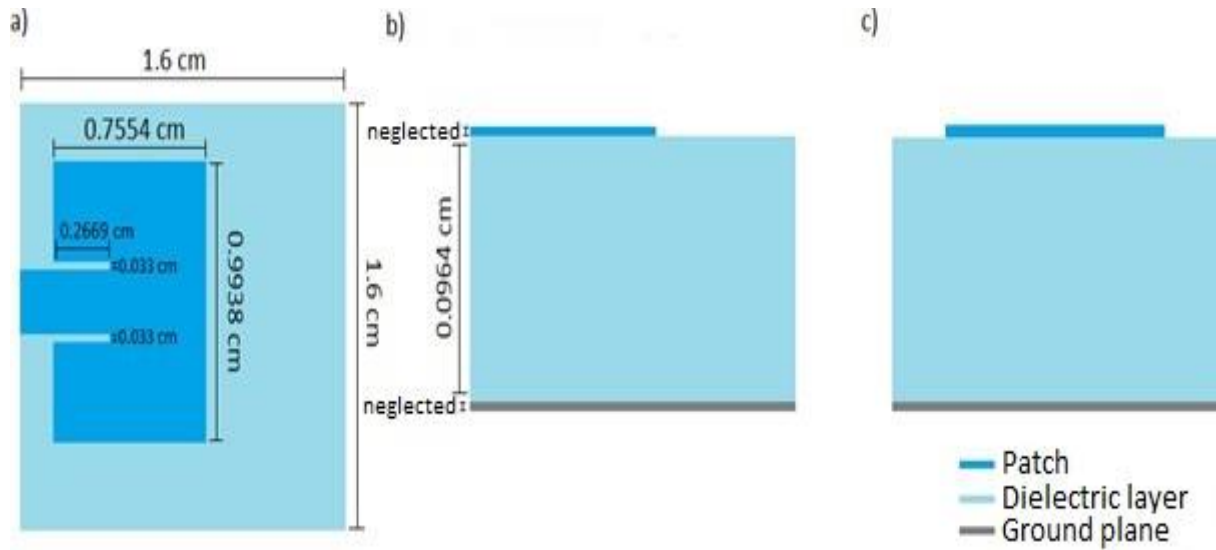


Figure 5: Schematic views of the designed antenna. a) XY (above) view b) YZ (side) view c) XZ (side) view.

3. Simulations

In this section, s11 reflection coefficient magnitude graphs, antenna input impedance graphs, radiation patterns for E plane and H plane and antenna gain graphs are drawn.

3.1 Plotting the S11 characteristic and showing the bandwidth by frequency in the range of 500 MHz below and above the operating frequency

S11 is a measure of how much power is reflected back at the antenna port due to mismatch from the transmission line [25]. When S11 is plotted between 500 MHz below and above the determined operating frequency of 10 GHz, as seen in Figure 6, the operating frequency of the antenna has changed due to the fringing areas. Fringing areas cause the effective length to change as mentioned before. Therefore, in HFSS, L length was manually changed and an L providing 10 GHz was obtained. Figure 7 describes the s11 reflection coefficient magnitude graph according to the frequency in the range 500 MHz below and above the operating frequency for the manually found L. After obtaining Figure 7, the bandwidth at -10 dB is found as in equation 10.

$$f_2 - f_1 = (10.1307 - 9.8475) (GHz) = 0.2832 GHz \quad (10)$$

The bandwidth was calculated as in equation 11. This complies with the requirement of design specifications that the -10dB bandwidth (BW) of the desired antenna should be at least 1.6%.

$$BW\% = [(f_2 - f_1)/10]100 = 2.83\% \quad (11)$$

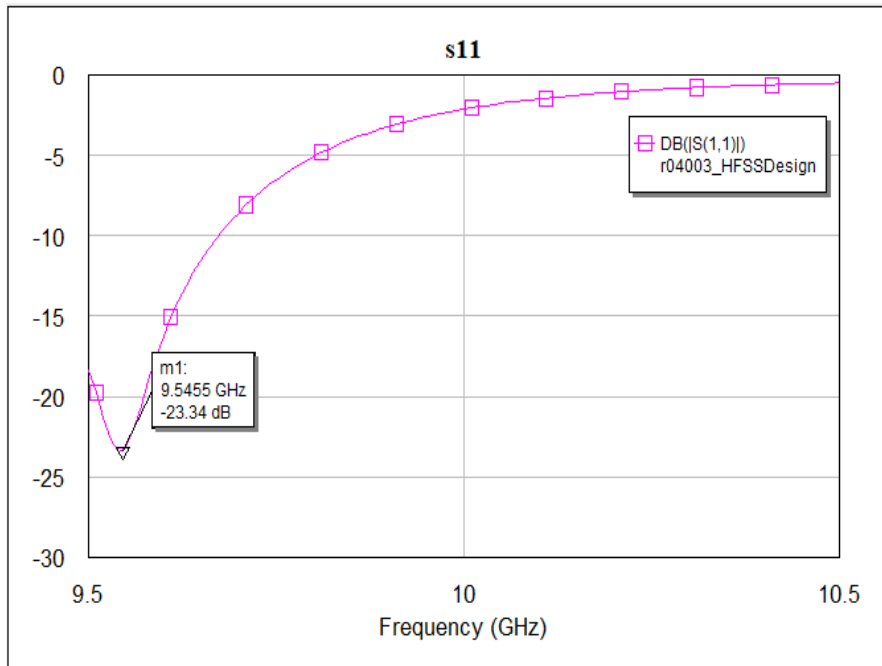


Figure 6: S_{11} characteristic according to the frequency in the range of 500 MHz below and above the operating frequency for the antenna according to section 3 and showing the bandwidth.

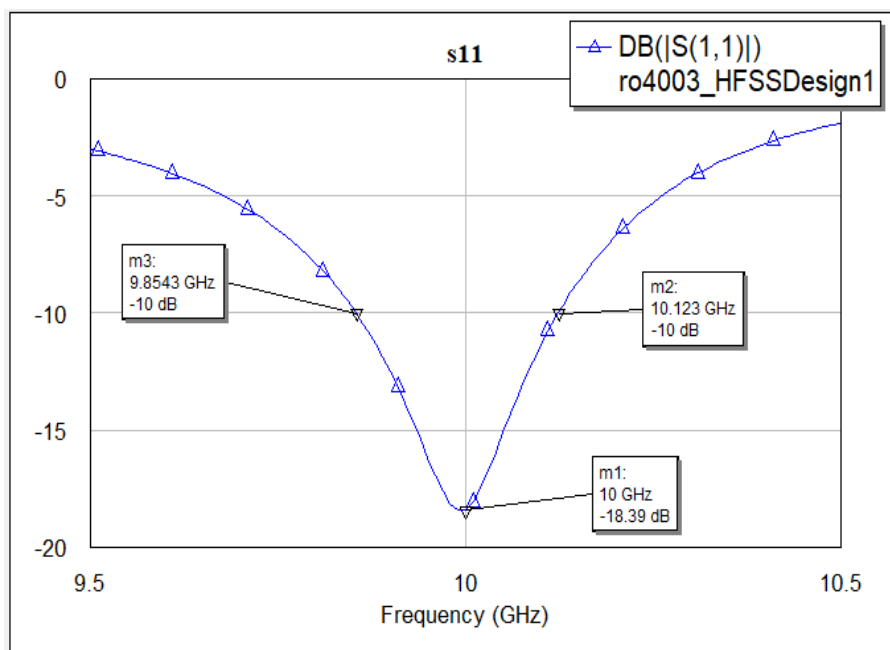


Figure 7: Plotting the S_{11} characteristic according to the frequency in the range 500 MHz below and above the operating frequency for the manually found L and showing the bandwidth.

3.2 Plotting antenna input impedance in the range 250 MHz below and above operating frequency

In Figure 8, the real graph, the imaginal graph and the magnitude graph of the antenna input impedance are plotted between 9.75 GHz and 10.25 GHz. As can be seen, at 10 GHz, the real impedance is 64Ω and the imaginal impedance is very close to zero. In general, it can be seen that the antenna input impedance is around 50Ω between 9.75-10.15 GHz.

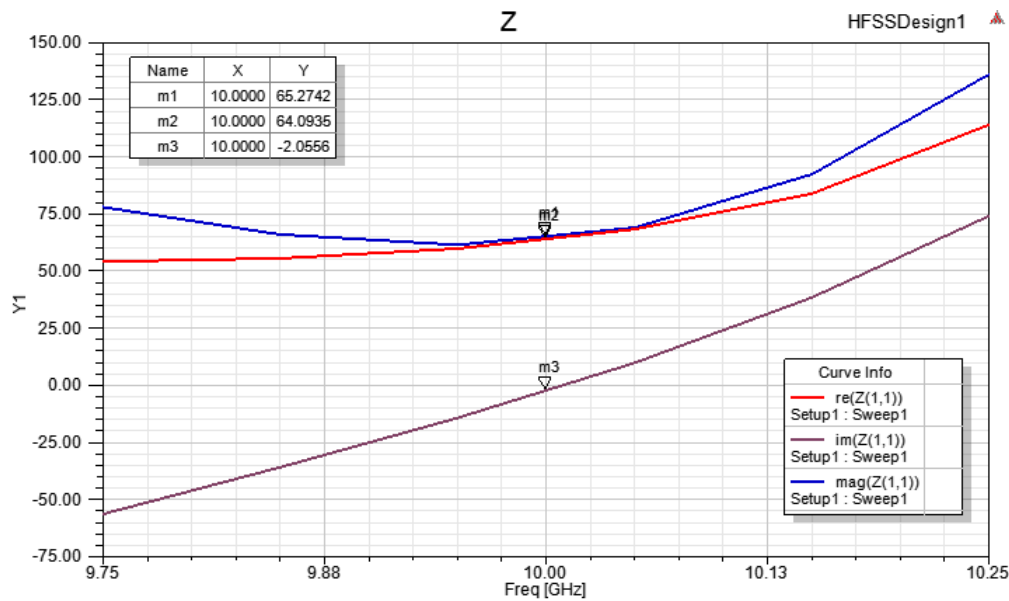


Figure 8: Antenna input impedance graph in the 9.75 GHz and 10.25 GHz range.

Figure 9 shows the impedance graph of the antenna's input port. For 9.75 GHz and 10.25 GHz, the real impedance is 50Ω and the imaginal impedance is 0 at all frequency values.

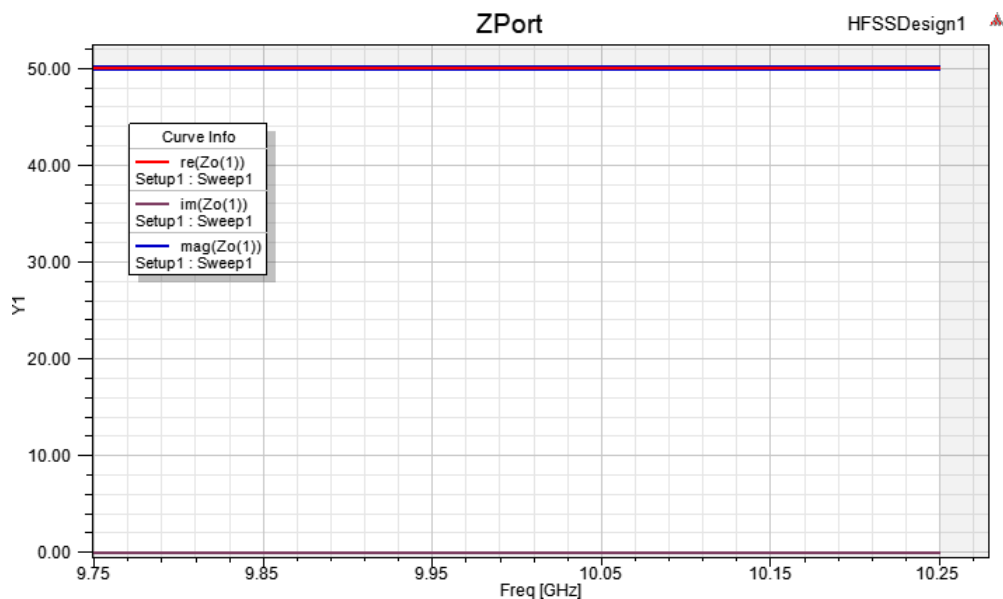


Figure 9: Impedance graph of antenna input port in the range of 9.75 GHz and 10.25 GHz.

3.3 Plotting the radiation pattern for the E-Plane and the H-Plane at 10 GHz operating frequency

Considering the direction of the electric field and the radiation direction, the E plane is the YZ plane, i.e. $\phi = \pi/2$ plane, and the H plane is the $\phi = 0$ plane. Considering these, radiation patterns at 10 GHz are drawn for E and H planes, respectively, in Figure 10 and Figure 11.

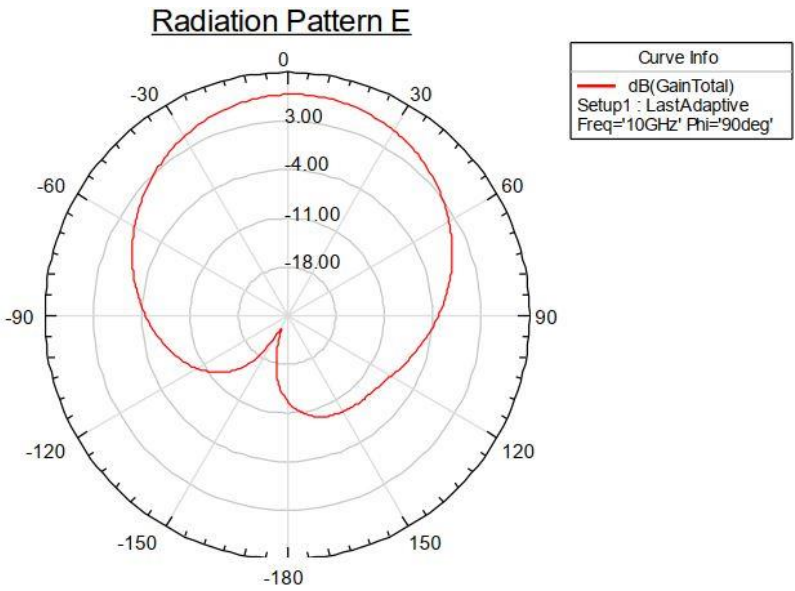


Figure 10: Radiation pattern for the E plane at operating frequency.

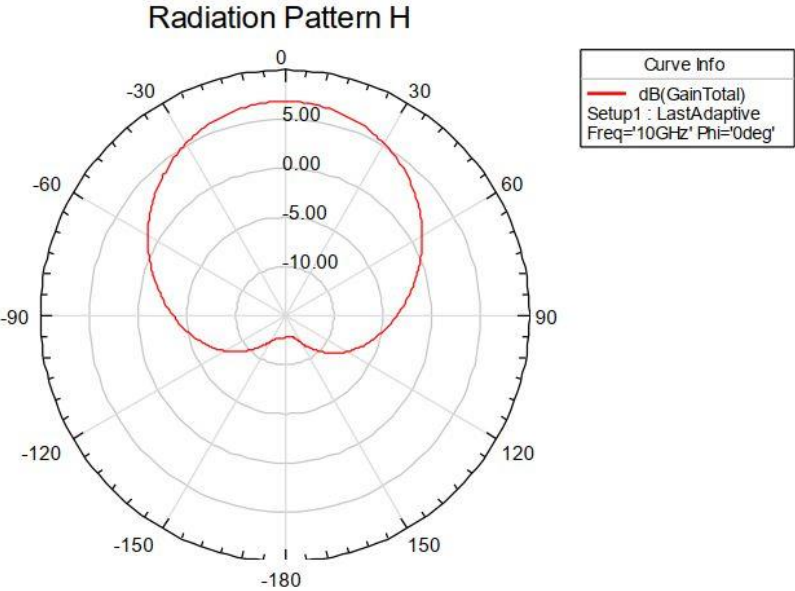


Figure 11: Radiation pattern for the H plane at operating frequency.

3.4 3D plotting of antenna gain at operating frequency

Antenna gain at 10 GHz is plotted in 3D in Figure 12. As can be seen from the Figure 12, the antenna gain is higher than 5 dB.

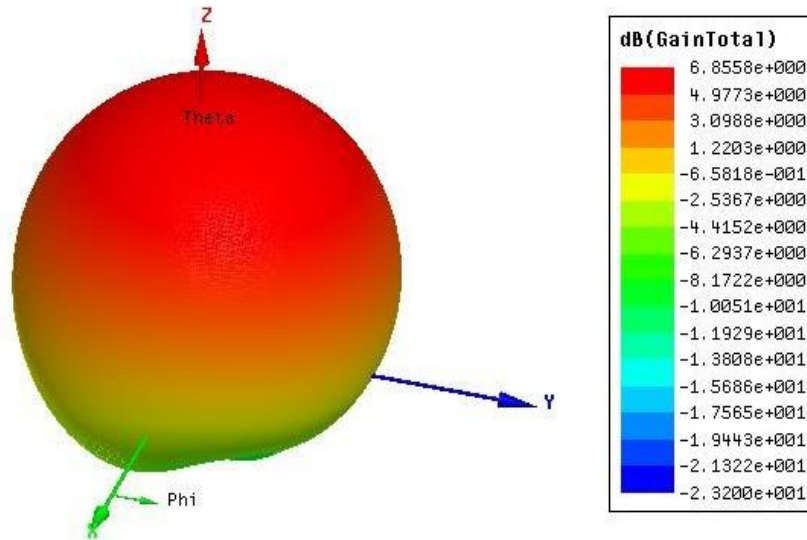


Figure 12: 3D antenna gain at operating frequency.

3.5 Plotting antenna gain at 250 MHz above and below operating frequency

Antenna gain in the 9.75 and 10.25 GHz range is plotted in Figure 13 depending on θ . As can be seen, the antenna gain is equal to 6.8 dB when $\theta = 0$.

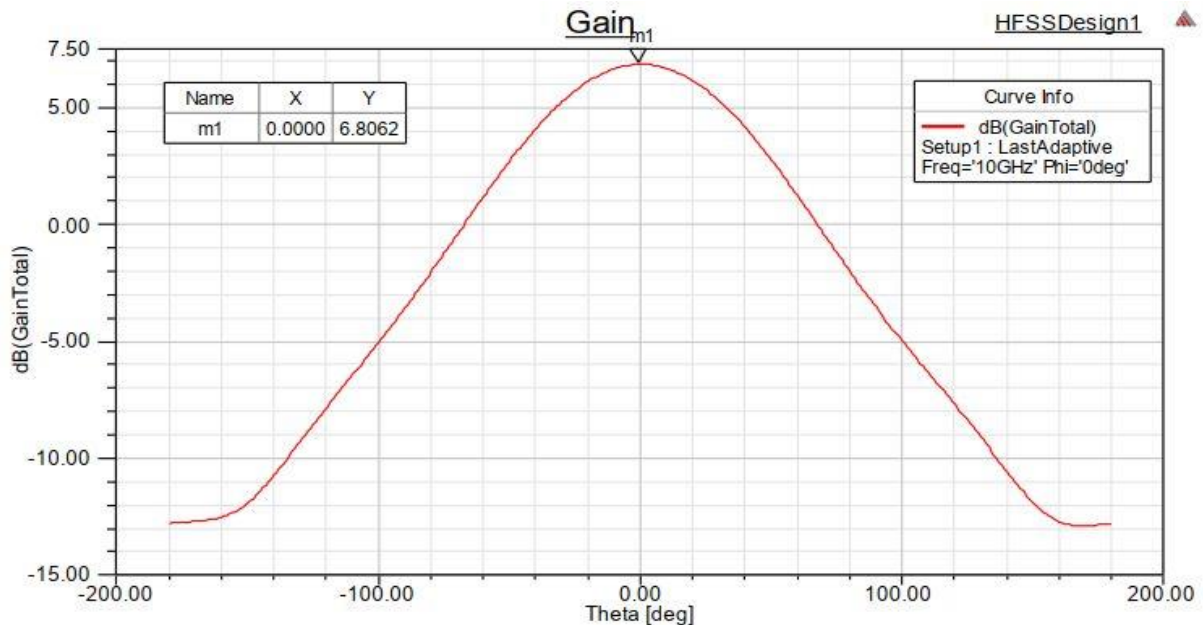


Figure 13: The graph of antenna gain connected to θ .

4. Conclusion

In this study, the design of a microstrip patch antenna at 10 GHz frequency for X band applications is explained. First of all, the usage areas, structure and working principles of the microstrip patch antenna are explained. HFSS, AWS and MATLAB programs were used in the antenna design. The equations used in this design are explained one by one. Using MATLAB program, these equations were solved and the values of the parameters were found. The schematic drawings of the antenna are given from the top and from the side. In the simulation section, S11 characteristic graphics, input impedance graphics, E and H plane radiation patterns and antenna gain graphics were drawn. The parameters used in the antenna design are presented in a table. Simulation results show that the antenna works as desired and meets the X Band design criteria.

References

- [1] Singh, I., & Tripathi, V. S. (2011). Micro strip patch antenna and its applications: a survey. *Int. J. Comp. Tech. Appl*, vol. 2(5), pp. 1595-1599.
- [2] Deepa, J., Santhanam, S., Vasudevan, N., & Chandran, S. S. (2022). Substrate integrated waveguide antenna with dual rectangular slots for material characterization for ISM band applications. *Materials Today: Proceedings*, vol. 69, pp. 1493-1497.
- [3] Bisht, S., Saini, S., Prakash, V., & Nautiyal, B. (2014). Study the various feeding techniques of microstrip antenna using design and simulation using CST microwave studio. *International Journal of Emerging Technology and Advanced Engineering*, vol. 4(9), pp. 318-324.
- [4] Shome, P. P., Khan, T., & Laskar, R. H. (2019). A state-of-art review on band-notch characteristics in UWB antennas. *International Journal of RF and Microwave Computer-Aided Engineering*, vol. 29(2), pp. e21518.
- [5] Mishra, R. (2016). An overview of microstrip antenna. *HCTL Open International Journal of Technology Innovations and Research (IJTIR)*, vol. 21(2), pp. 39-55.
- [6] Karahan, M., & Kasnakoglu, C. (2021). Modeling a Quadrotor Unmanned Aerial Vehicle and robustness analysis of different controller designs under parameter uncertainty and noise disturbance. *Control Engineering and Applied Informatics*, vol. 23(4), pp. 13-24.
- [7] Rana, M. S., & Rahman, M. M. (2022). Study of microstrip patch antenna for wireless communication system. In *2022 International Conference for Advancement in Technology (ICONAT)*, (pp. 1-4). IEEE.
- [8] Colaco, J., & Lohani, R. (2020). Design and Implementation of microstrip patch antenna for 5G applications. In *2020 5th International Conference on Communication and Electronics Systems (ICCES)*, (pp. 682-685). IEEE.
- [9] Kiani, N., Hamedani, F. T., & Rezaei, P. (2021). Polarization controlling plan in graphene-based reconfigurable microstrip patch antenna. *Optik*, 244, 167595.
- [10] Hocini, A., Temmar, M. N., Khedrouche, D., & Zamani, M. (2019). Novel approach for the design and analysis of a terahertz microstrip patch antenna based on photonic crystals. *Photonics and Nanostructures-Fundamentals and Applications*, 36, 100723.
- [11] Wang, X., Wu, L., Chen, H., Wang, W., & Liu, Z. (2023). Frequency-Reconfigurable Microstrip Patch Antenna Based on Graphene Film. *Electronics*, 12(10), 2307.

- [12] Ghimire, J., Khan, D., & Choi, D. Y. (2023). Microstrip to Slot-Line-Fed Microstrip Patch Antenna with Radiation Pattern Diversity for X-Band Application. *Electronics*, 12(17), 3672.
- [13] Benlakehal, M. E., Hocini, A., Khedrouche, D., Temmar, M. N., Denidni, T. A., & Shayea, I. (2023). Design and analysis of a 1×2 microstrip patch antenna array based on photonic crystals with a graphene load in THZ. *Journal of Optics*, 52(2), 483-493.
- [14] Ihamji, M., Abdelmounim, E., Bennis, H., & Latrach, M. (2019). Design of miniaturized antenna for RFID applications. In *Emerging Innovations in Microwave and Antenna Engineering*, (pp. 325-362). IGI Global.
- [15] Varshney, A., & Sharma, V. (2020). A comparative study of microwave rectangular waveguide-to-microstrip line transition for millimeter wave, wireless communications and radar applications. *Microw. Rev*, 2(26), 26-37.
- [16] Mishra, B., Verma, R. K., Yashwanth, N., & Singh, R. K. (2022). A review on microstrip patch antenna parameters of different geometry and bandwidth enhancement techniques. *International Journal of Microwave and Wireless Technologies*, 14(5), 652-673.
- [17] Lee, C. S., Bai, B., Song, Q. R., Wang, Z. Q., & Li, G. F. (2019). Open complementary split-ring resonator sensor for dropping-based liquid dielectric characterization. *IEEE Sensors Journal*, 19(24), 11880-11890.
- [18] Hashim, F. F., Mahadi, W. N. L. B., Abdul Latef, T. B., & Othman, M. B. (2022). Key Factors in the Implementation of Wearable Antennas for WBNs and ISM Applications: A Review WBNs and ISM Applications: A Review. *Electronics*, vol. 11(15), pp. 2470.
- [19] Ashraf, S., Sheikh, J. A., Ashraf, A., & Rasool, U. (2023). Comparative analysis of rectangular framed S-shaped millimeter-wave antenna for different feeding techniques. *Materials Today: Proceedings*, 74, 123-129.
- [20] Kashyap, N., Singh, D., & Sharma, N. (2022). Comprehensive Study of Microstrip Patch Antenna Using Different Feeding Techniques. *ECS Transactions*, 107(1), 9545.
- [21] Yan, J., Stevens, C. J., & Shamonina, E. (2021). A metamaterial position sensor based on magnetoinductive waves. *IEEE Open Journal of Antennas and Propagation*, 2, 259-268.
- [22] Al Ahmad, M., Kabeer, S., Sanad, A. A., & Olule, L. J. (2021). Compact single-varactor diode frequency-reconfigurable microstrip patch antenna. *IET Microwaves, Antennas & Propagation*, 15(9), 1100-1107.
- [23] Khan, A., & Nema, R. (2012). Analysis of five different dielectric substrates on microstrip patch antenna. *International journal of computer applications*, vol. 55(14).
- [24] Vishnu Chandar, J., Mutharasu, D., Mohamed, K., Marsilla, K. I. K., Shanmugan, S., & Azlan, A. A. (2021). Melt compounded polylactic acid-hexagonal boron nitride-aluminum oxide hybrid composites for electronic applications: impact of hybrid fillers on thermophysical, dielectric, optical, and hardness properties. *Polymer-Plastics Technology and Materials*, 60(2), 147-164.
- [25] Iqbal, A., Al-Hasan, M., Mabrouk, I. B., Basir, A., Nedil, M., & Yoo, H. (2021). Biotelemetry and wireless powering of biomedical implants using a rectifier integrated self-diplexing implantable antenna. *IEEE Transactions on Microwave Theory and Techniques*, vol. 69(7), pp. 3438-3451.